# Ordering and metastable state during the growth of fcc alloy monolayers

Hongting Shi and Jun Ni
*Department of Physics, Tsinghua University, Beijing 100084, China*
(Received 8 October 2001; published 8 March 2002)

The kinetics of ordering in fcc alloys during the growth of a (001) monolayer is investigated by the kinetic mean-field method. The evolution of the structure parameters is calculated. There is a transient ordered state during the growth process and its occurrence depends on the ratio of the atomic exchange rate to the evaporation rate. The growth process displays two stages of evolution. The first stage is the formation of a metastable ordered state whose lifetime increases exponentially with the decrease of the temperature. The second stage is the evolution from the metastable ordered state to the equilibrium ordered state. The stoichiometric concentrations of the metastable ordered state is found to be different from the equilibrium one. The influence of the two characteristic times related to the adsorption and the atomic migration on the kinetics of the growth is analyzed.

DOI: 10.1103/PhysRevB.65.115422 PACS number(s): 64.60.Cn, 64.60.My, 82.40.Bj

## I. INTRODUCTION

Epitaxial growth has been used with layer-by-layer control over growth of materials. It is found that III-V semiconductor alloys exhibit long-range order[1–5] when grown by the epitaxial method despite the fact that the bulk phase diagram predicts phase separation at growth temperature. Epitaxial metal alloy shows various ordering behavior.[6,7] The amount of long-range order and its presence depend sensitively on the growth conditions. Saito and Müler-Krumbhaar[8] used a kinetic mean-field theory in pair approximation to discuss the crystal growth. Venkatasubramanian[9] developed the kinetic mean-field model to treat the growth of an alloy with short-range order. Smith and Zangwill[10] used the kinetic mean field to study the interplay between compositional ordering and surface roughening during the epitaxial growth of a binary alloy. The Monte Carlo method has also been used to simulate the growth of phase separating alloys[11,12] and ordering alloys[13,14] on the morphology and the scaling behavior of the system.

The epitaxial growth of alloys is a nonequilibrium process controlled by various relaxation processes such as the surface diffusion, adsorption, and evaporation. It was shown that transient ordered states can be formed in various systems during the relaxation of a nonequilibrium state to the equilibrium state.[15–18] The occurrence of these transient ordered states is due to the multiple characteristic times during the relaxation process. When the evolution of the system is controlled by the multiple relaxation rates, the system can first reach a kind of transient state through the kinetics process with faster relaxation rate. This transient state is a relative stable state. As other relaxation processes become functional, the system gradually relaxes to the equilibrium state. In the kinetics of ordering in alloys, there are multiple characteristic times for the atomic migration that control the relaxation of different atomic species, which leads to transient states on its relaxation path to the final equilibrium phase.[17,18] For epitaxial growth, in addition to the diffusion process, there are other two relaxation processes: i.e., the adsorption and evaporation process. This can result in transient and metastable states in the growth process due to multiple relaxation times.

In this paper, we study the kinetics of ordering in alloys during a monolayer growth. The evolution of the concentrations and order parameters during the growth is calculated. We will show that there are transient and metastable ordered states in the system during the growth. The influence of the growth parameters on the kinetic process is discussed.

In Sec. II we describe the methods. Section III presents the results of the kinetics of ordering during the growth. Section IV is the conclusions.

## II. METHODS

We consider the growth layer of an fcc alloy in the (001) direction. The system consists of three components: two species of $A$ and $B$ atoms and vacancy ($V$) on the growth layer. The surface of an fcc alloy is a square lattice as shown in Fig. 1. To describe the ordering of the system with nearest-neighbor and next-nearest-neighbor interactions, we divide the lattice into four sublattices. In the mean-field approximation, the configurations of the system are described by the site probabilities. $P_i^s$ is the probability occupied by $i$ $(=A,B,V)$ species in $s(\alpha,\beta,\gamma,\delta)$ sublattices on the growth layer at time $t$. Here $P_i^s$ satisfies the normalization condition $\Sigma_{i=A,B,V}P_i^s(t)=1$. We consider the nearest-neighbor and next-nearest-neighbor interactions of atoms in the growth process. Then the atoms in the growth layer have the interactions with the first two layers of the substrate. The growth

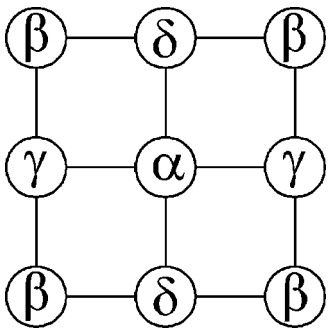


FIG. 1. Four square sublattices $\alpha$, $\beta$, $\gamma$, and $\delta$ for the (001) codeposition layer.

 

process comprises the three relaxation processes such as the surface diffusion, adsorption, and evaporation processes.[8] In the following, we will describe the calculation of these three processes.

### A. Atomic diffusion process

We assume that surface atoms migrate by means of the surface diffusion whereby an *A* or *B* atom jumps to an empty nearest-neighbor adsorption site. We use the micromaster equation method[18–20] to describe the atomic diffusion process. We can define the basic exchange probability function $Y_{ij}^{ss'}(t)$. It represents the exchange probability between *i* species on sublattice *s* and *j* species on sublattice *s'* (one of them is a vacancy *V*) in unit time. We consider only the nearest-neighbor exchanges. There are 16 varieties of $Y_{ij}^{ss'}$. We take $Y_{ij}^{\alpha\gamma}$ as an example to show the evaluation of $Y_{ij}^{ss'}$. Here $Y_{ij}^{\alpha\gamma}$ is proportional to the characteristic exchange rate $\nu_{ij}$, the energy barrier factor $\exp(-\beta U_{ij})$, the site probabilities $P_i^{\alpha}$ and $P_i^{\gamma}$, and the bond broken factor for the atom-vacancy exchange $w_{ij}^{\alpha\gamma}$. Then $Y_{ij}^{\alpha\gamma}$ is given by

$$Y_{ij}^{\alpha\gamma}=P_i^{\alpha}P_j^{\gamma}w_{ij}^{\alpha\gamma}\nu_{ij}\exp\left(\frac{U_{ij}}{k_BT}\right), \tag{1}$$

where $U_{ij}=U_0+\Delta E_{ij}/2$ is the energy barrier for the atom-vacancy exchange. $U_0$ is the average barrier height for the atomic interchange. $\Delta E_{ij}$ is the energy difference for the atom-vacancy interchange. Each basic atom-vacancy exchange is affected by the interactions with the species on the neighboring 18 sites if we consider only nearest-neighbor and next-nearest-neighbor interactions. There is an factor $\exp(-\Delta E_{ij}/2k_BT)$ due to the influence of the neighboring species on the exchange. The bond broken factor $w_{ij}^{\alpha\gamma}$ is given by

$$\begin{aligned}
w_{ij}^{\alpha\gamma}=&\left[\sum_k P_k^{\beta}\exp\left(\frac{-1}{2k_BT}(E_{jk}^{(2)}-E_{ik}^{(2)})\right)\right]^2\left[\sum_k P_k^{\delta}\exp\left(\frac{-1}{2k_BT}(E_{ik}^{(2)}-E_{jk}^{(2)})\right)\right]^2\left[\sum_k P_k^{\gamma}\exp\left(\frac{-1}{2k_BT}(E_{jk}^{(1)}-E_{ik}^{(1)})\right)\right]\\
&\times\left[\sum_k P_k^{\alpha}\exp\left(\frac{-1}{2k_BT}(E_{ik}^{(1)}-E_{jk}^{(1)})\right)\right]\left[\sum_k P_k^{\delta}\exp\left(\frac{-1}{2k_BT}(E_{jk}^{(1)}-E_{ik}^{(1)})\right)\exp\left(\frac{-1}{2k_BT}(E_{ik}^{(2)}-E_{jk}^{(2)})\right)\right]^2\\
&\times\left[\sum_k P_k^{\beta}\exp\left(\frac{-1}{2k_BT}(E_{ik}^{(1)}-E_{jk}^{(1)})\right)\exp\left(\frac{-1}{2k_BT}(E_{jk}^{(2)}-E_{ik}^{(2)})\right)\right]^2\left[\sum_k P_k^{(1)\alpha}\exp\left(\frac{-1}{2k_BT}(E_{jk}^{(1)}-E_{ik}^{(1)})\right)\right]\\
&\times\left[\sum_k P_k^{(1)\delta}\exp\left(\frac{-1}{2k_BT}(E_{jk}^{(1)}-E_{ik}^{(1)})\right)\right]\left[\sum_k P_k^{(1)\alpha}\exp\left(\frac{-1}{2k_BT}(E_{ik}^{(1)}-E_{jk}^{(1)})\right)\right]\left[\sum_k P_k^{(1)\delta}\exp\left(\frac{-1}{2k_BT}(E_{ik}^{(1)}-E_{jk}^{(1)})\right)\right]\\
&\times\left[\sum_k P_k^{(2)\alpha}\exp\left(\frac{-1}{2k_BT}(E_{jk}^{(2)}-E_{ik}^{(2)})\right)\right]\left[\sum_k P_k^{(2)\gamma}\exp\left(\frac{-1}{2k_BT}(E_{ik}^{(2)}-E_{jk}^{(2)})\right)\right],
\end{aligned} \tag{2}$$

where $E_{ij}^{(k)}$ ($k=1,2$ for the first- and second-nearest-neighbors, respectively) is the pair interaction energy between the *i* and *j* atoms. $P_k^{(i)s}$ represents the site probability of *k* species in the sublattice *s* on the substrate layer *i* ($i=1,2$). They are constant in the growth process. We can get other $w_{ij}^{ss'}$ similarly.

### B. Evaporation

We define $Z_i^s(t)$ as the evaporation probability per unit time of the *i* species from the *s* sublattice at time *t*. Here $Z_i^s$ is proportional to the characteristic evaporation rate $w_i$, the site probability $P_i^s$ of the evaporation atom, the chemical potential factor $\exp(-\mu_i/k_BT)$ ($\mu_i$ is the chemical potential of the *i* species), and the bond broken factor for the evaporation $V_i^s$. $Z_i^s$ is given as follows:

$$Z_i^s(t)=-w_iV_i^sP_i^s\exp\left(\frac{-\mu_i}{k_BT}\right). \tag{3}$$

The negative sign means that it contributes to the decrease of $P_i^s$. The evaporation atoms have binding interactions with the neighboring atoms and these binding energies need to be overcome for the evaporation. This leads to the bond broken factor for the evaporation $V_i^s$ which is given as

$$\begin{aligned}
V_i^{\alpha}=&\left[\sum_k P_k^{\beta}\exp\left(\frac{E_{ik}^{(2)}}{k_BT}\right)\right]^4\left[\sum_k P_k^{\gamma}\exp\left(\frac{E_{ik}^{(1)}}{k_BT}\right)\right]^2\\
&\times\left[\sum_k P_k^{\delta}\exp\left(\frac{E_{ik}^{(1)}}{k_BT}\right)\right]^2\left[\prod_{\nu}\sum_k P_k^{(1)\nu}\exp\left(\frac{E_{ik}^{(1)}}{k_BT}\right)\right]\\
&\times\left[\sum_k P_k^{(2)\alpha}\exp\left(\frac{E_{ik}^{(2)}}{k_BT}\right)\right].
\end{aligned} \tag{4}$$

$V_i^{\beta}$, $V_i^{\gamma}$, and $V_i^{\delta}$ can be calculated similarly.

### C. Adsorption

We define $X_i^s(t)$ as the adsorption probability per unit time of the *i* species on the *s* sublattice at time *t*. Here $X_i^s$ is

proportional to the characteristic adsorption rate $w_i'$, the chemical potential factor $\exp(\mu_i/k_BT)$, and the vacancy probability $P_V^s$:

$$X_i^s = w_i' P_V^s \exp\left(\frac{\mu_i}{k_B T}\right). \tag{5}$$

In this form of the adsorption probability, the characteristic adsorption rate $w_i'$ is equal to the characteristic evaporation rate $w_i$ due to the detailed balance condition between the evaporation and the adsorption.

### D. Kinetic equations

From the above analysis, we can get the following differential equations describing the kinetics of growth by including all the three contributions from the atom-vacancy exchange, evaporation, and adsorption processes:

$$\frac{d}{dt}P_i^\alpha = 2[Y_{Vi}^{\alpha\gamma} - Y_{iV}^{\alpha\gamma}] + 2[Y_{Vi}^{\alpha\delta} - Y_{iV}^{\alpha\delta}] + Z_i^\alpha + X_i^\alpha,$$

$$\frac{d}{dt}P_i^\beta = 2[Y_{Vi}^{\beta\gamma} - Y_{iV}^{\beta\gamma}] + 2[Y_{Vi}^{\beta\delta} - Y_{iV}^{\beta\delta}] + Z_i^\beta + X_i^\beta,$$

$$\frac{d}{dt}P_i^\gamma = 2[Y_{iV}^{\alpha\gamma} - Y_{Vi}^{\alpha\gamma}] + 2[Y_{iV}^{\beta\gamma} - Y_{Vi}^{\beta\gamma}] + Z_i^\gamma + X_i^\gamma,$$

$$\frac{d}{dt}P_i^\delta = 2[Y_{iV}^{\alpha\delta} - Y_{Vi}^{\alpha\delta}] + 2[Y_{iV}^{\beta\delta} - Y_{Vi}^{\beta\delta}] + Z_i^\delta + X_i^\delta. \tag{6}$$

The growth process is described by the concentrations of the atomic species and the order parameters. The atomic configurations is determined by the occupation probability $P_i^s$ of $i$ species ($i=A,B,V$) in the sublattice $s$. The symmetry of the atomic configurations of the phases are generally described by the following independent order parameters related to the site probability $P_i^s$:

$$\gamma_1^i = P_i^\alpha + P_i^\beta - P_i^\gamma - P_i^\delta,$$

$$\gamma_2^i = P_i^\alpha - P_i^\beta,$$

$$\gamma_3^i = P_i^\gamma - P_\nu^\delta \tag{7}$$

where $i=A$ and $B$. The order parameter $\gamma_1^i$ indicates the atomic configuration between the nearest-neighbor sites of species $i$. Similarly, other order parameters $\gamma_2^i$ and $\gamma_3^i$ show the atomic configurations between the second-nearest-neighbor sites. The values of these parameters define the following phases with different symmetry: (1) disordered phase: $\gamma_k^i=0$; (2) $O_1$: $\gamma_1^i\neq 0$, $\gamma_2^i=\gamma_3^i=0$; (3) $O_2$: $\gamma_1^i=0$, $\gamma_2^i\neq 0$, $\gamma_3^i\neq 0$. The concentrations are related to the site probability $P_i^s$ as follows:

$$C_i = \frac{1}{4}(P_i^\alpha + P_i^\beta + P_i^\gamma + P_i^\delta). \tag{8}$$

The coverage of the layer is the sum of the concentration of the atomic species. The differential equations are solved numerically by the Runge-Kutta method. Initially the growth is empty. The growth process is described by the evolution of the concentrations and the order parameters governed by the above differential equations.

## III. RESULTS

In our calculations, we consider the first- and second-nearest-neighbor interactions. Only the first two layers of the substrate have an influence on the growth process. The configurations of the substrate are fixed. During the growth, the temperature $T$ and the chemical potentials which control the concentrations of the atomic species are kept constant. At $t=0$, the coverage of the two atomic species is zero. We have calculated the kinetics of ordering during the growth with the variation of the growth parameters. For the ordering of the codeposition layer of fcc metal alloys and III-V semiconductor alloys, generally four sublattices are needed to describe the ordered phases on the codeposition layer and there are two kinds of ordered phases $O_1$ and $O_2$ described by the four sublattices. Both first- and second-nearest-neighbor interactions should be considered for the formation of these ordered phases. For the codeposition layer of the metal alloys with CuAu-like structure, the ordered phase is $O_1$ which favors the first-nearest neighbor bonds of different species. Many epitaxial III-V semiconductor alloys showing $L1_1$ (CuPt-like) superstructures,[11] the structure of (001) codeposition layer is $O_2$ which favors the second-nearest-neighbor bonds of different species. In order to comprehend the kinetics of ordering during the growth process for the system with the ordered phases $O_1$ and $O_2$, we have taken the energy parameters exhibiting ordered phases $O_1$ and $O_2$, respectively. The types of kinetic path for the growth corresponding to the ordered phases $O_1$ and $O_2$ are calculated. In order to investigate the effects of the kinetic parameters (such as temperature and the characteristic times) on kinetics of the growth, the evolutions of the structure with the variation of the kinetic parameters are calculated. For the ordered phase $O_1$, the interaction energies are taken as $E_{AB}^{(1)}=-0.6$, $E_{AA}^{(1)}=E_{BB}^{(1)}=-0.1$, and $E_{AB}^{(2)}=-0.1$, $E_{AA}^{(2)}=E_{BB}^{(2)}=-0.6$. For the ordered phase $O_2$, the interaction energies are taken as $E_{AB}^{(1)}=-0.1$, $E_{AA}^{(1)}=E_{BB}^{(1)}=-0.6$, and $E_{AB}^{(2)}=-0.6$, $E_{AA}^{(2)}=E_{BB}^{(2)}=-0.1$. We take $\nu_{AV}=\nu_{BV}$ and denote $\tau_D=\nu_D^{-1}\equiv\nu_{AV}$. The barrier energies are taken as $V_{AC}=V_{BC}=0.6$.

Figure 2 shows the evolution of the concentrations and the order parameters for the ordered phase $O_1$. The structure of the substrate is taken as ordered one. Since the atomic interactions favor the $AA$ and $BB$ atom pairs of the second-nearest-neighbor between the second-nearest-neighboring layers, the order parameters of the growth layer have the same signs with those of the second layer of the substrate. The structure of the first substrate layer has no influence on the ordered parameters of the growth layer because each lattice site of the growth layer has the first-nearest-neighbor interactions with the lattice sites of all the four sublattices of the first substrate layer. Therefore, the second-nearest-neighbor interactions determine the stacking structure along the growth direction. Figure 3 shows the evolution of the

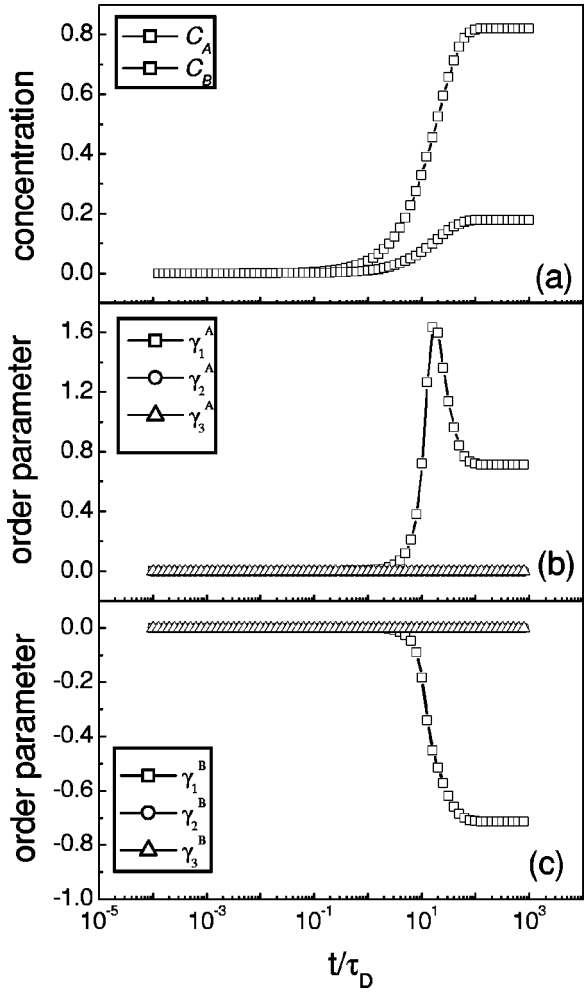


FIG. 2. Evolution of the structure parameters during the growth for the ordered phase $O_1$ at the temperature $k_BT=0.3$ and the chemical potentials $\mu_A=0.5$ and $\mu_B=0.25$. Here $w_A/\nu_D=1/8$ and $w_B/\nu_D=1/16$. (a) Curves for concentrations, (b) curves for $\gamma_1^A$, and $\gamma_2^A$, and $\gamma_3^A$, and (c) curves for $\gamma_1^B$, $\gamma_2^B$, and $\gamma_3^B$.

concentrations and order parameters for the ordered phase $O_2$. The atomic interactions favor the $A$ and $B$ atom pair of the second-nearest-neighbor between the second-nearest-neighboring layers. The order parameters of the growth layer have the opposite signs with those of the second layer of the substrate. From the figure, we can see that the kinetic process has the similar features as that for the ordered phase $O_1$.

### A. Effects of the characteristic rates

The evolutions of the site probabilities of $A$ atoms on the sublattices $\gamma$ and $\delta$ have fluctuation during the growth process. There is a peak in the evolution curves. The mechanism for the occurrence of the peak is as follows: Due to the ordering effect, there are migrations of the $A$ atoms among different sublattices. When there are more $A$ atoms jumping from the sublattices $\gamma$ and $\delta$ to the sublattices $\alpha$ and $\beta$ than $A$ atoms deposited onto the sublattices $\gamma$ and $\delta$, the decrease of the site probabilities of $A$ atoms on the sublattices $\gamma$ and $\delta$ occurs. This phenomenon is due to the existence of the two

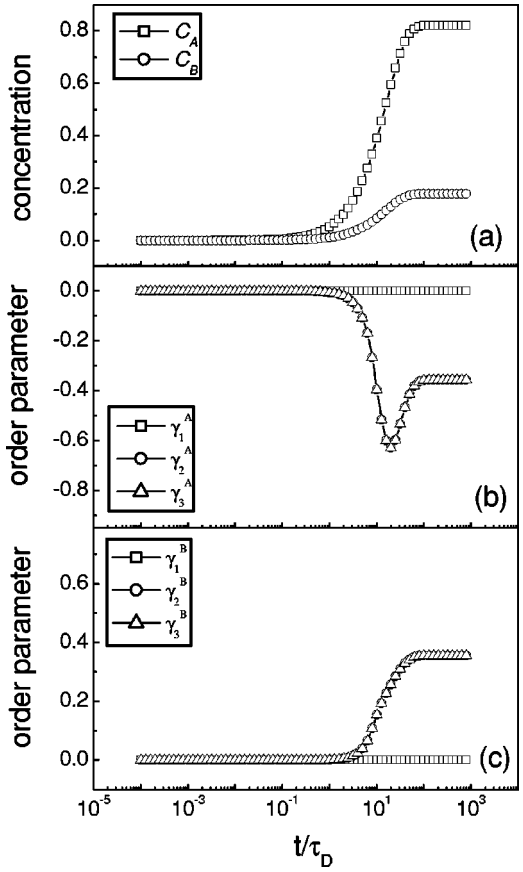


FIG. 3. Evolution of the structure parameters during the growth for ordered phase $O_2$ at the temperature $k_BT=0.3$ and the chemical potentials $\mu_A=0.5$ and $\mu_B=0.25$. Here $w_A/\nu_D=5/4$ and $w_B/\nu_D=5/8$. (a) Curves for concentrations, (b) curves for $\gamma_1^A$, $\gamma_2^A$, and $\gamma_3^A$, and (c) curves for $\gamma_1^B$, $\gamma_2^B$ and $\gamma_3^B$.

different kinetic processes controlled by two characteristic rates: i.e., the characteristic exchange rate and the characteristic adsorption rate. From our calculations, the peak occurs only within certain range of the ratio between the characteristic exchange rate and the characteristic adsorption rate. When the characteristic exchange rate is small enough that the adsorption rate of atoms on a sublattice is always larger than the migration rate of atoms, the site probabilities on the sublattice will always increase to approach the equilibrium values. Otherwise, when the characteristic exchange rate is large, the atomic migrations are very fast during the growth process and the configuration of the atoms is always in a relative equilibrium state in a certain time $t$. The site probabilities in each sublattice in a certain time $t$ describe such a quasiequilibrium state and thus there is no peak in the curve of the site probabilities for the case of large characteristic exchange rate. In a constant-temperature process, the exchange rate and the adsorption rate are proportional to the exponential terms of the energy barrier and chemical potentials. These terms are the controlling factors of the process. The results show that the peak in the evolution of the site probability occurs only when the difference between the characteristic exchange rate and the characteristic adsorption rate is small. For the evolution of order parameters as shown

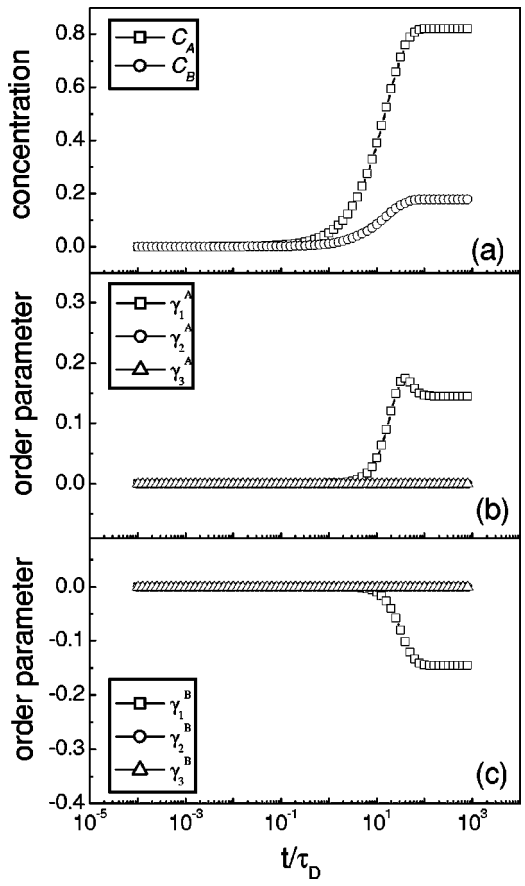


FIG. 4. Evolution of the structure parameters during the growth for the ordered phase $O_1$ at the temperature $k_BT=0.3$ and the chemical potentials $\mu_A=0.5$ and $\mu_B=0.25$. Here $w_A/\nu_D=5/4$ and $w_B/\nu_D=5/8$. (a) Curves for concentrations, (b) curves for $\gamma_1^A$, $\gamma_2^A$, and $\gamma_3^A$, and (c) curves for $\gamma_1^B$, $\gamma_2^B$, and $\gamma_3^B$.

in Figs. 2(b) and 2(c), it can be seen that there is a transient state in the growth process. The order parameter $\gamma_A$ changes from zero to a maximum value and then the order parameter changes from the maximum value to the equilibrium value. The peak of the order parameter $\gamma_A$ corresponds to those of the site probabilities of $A$ atoms on the sublattices $\gamma$ and $\delta$.

Figure 4 shows the evolution of the order parameters for a smaller characteristic exchange rate. The other growth parameters are taken to be same as those of Fig. 2 for comparison. As shown in Fig. 4, both the peak value and the equilibrium value of the order parameter $\gamma_A$ are smaller than those of Fig. 2. When the atomic migration rate is slow, the atoms have less time to adjust their configuration. Since the concentration of vacancy decreases exponentially as the growth proceeds, the diffusion rates for the atomic species $A$ and $B$ become very small due to the low vacancy concentration in the late stage of the growth and the atomic configuration become frozen up. The system relaxes to a metastable state with smaller order parameters. In the next subsection, we will show that the system will relax to the equilibrium state if the growth time is long enough, but the relaxation time to the equilibrium ordered state increases exponentially with the decrease of the temperature.

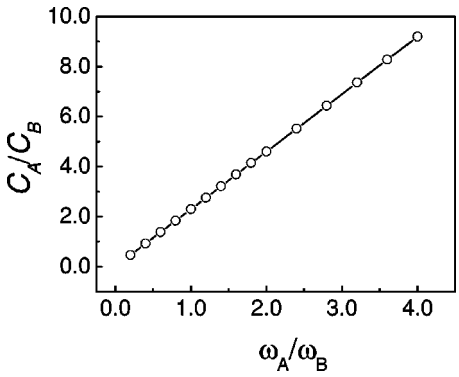


FIG. 5. The ratio of the concentrations of the $A$ and $B$ species as a function of the ratio of the characteristic adsorption rates of the $A$ and $B$ species. The numerical result is drawn as dot line and Eq. (9) is drawn as solid line.

The concentrations of the atomic species on the growth layer depend on the characteristic adsorption rate, chemical potentials, and growth temperature. Figure 5 shows the ratio of the concentrations of $A$ atoms and $B$ atoms for the metastable state as a function of the ratio of two characteristic atomic evaporation rates at the temperature $k_BT=0.3$. The ratio of the two atomic concentrations for the metastable state satisfies the following relation:

$$\frac{C_A}{C_B}=\frac{w_A\exp(\mu_A/k_BT)}{w_B\exp(\mu_B/k_BT)}. \tag{9}$$

The dotted line is the numerical result which is in good agreement with solid line for Eq. (9). Equation (9) shows that the relation between the concentrations of the species $A$ and $B$ is determined by the adsorption process. With the increase of temperature, the effect of evaporation will be more significant. Since the grown state is a metastable one, it will develop to the equilibrium state with the increase of the growth time and the ratio between the two atomic concentrations will approach to that for the equilibrium state.

### B. Influence of temperature

We have investigated the evolution of the order parameters and the concentrations during the growth process with the variation of temperature. The results for the temperature $k_BT=0.6$ is shown in Fig. 6. For comparison, the other parameters except the temperature are taken to be same as those in Fig. 2. As shown in Fig. 6, there are two stages of evolution in the growth process. In the first stage, the ordered phase $O_1$ has smaller order parameters. The kinetic process is similar with that in low temperature shown in Fig. 2. In the second stage, the system relaxes to an ordered phase with higher long-range order. The site probabilities of the $A$ atoms on the $\gamma$ and $\delta$ sublattices increase in the beginning of the first stage and then settle to the steady values. In the second stage of the growth process, the site probabilities of the $A$ atoms on the $\gamma$ and $\delta$ sublattices decrease to the equilibrium values while the site probabilities of the $B$ atoms increase. This leads to an increase of the order parameters. The curve of concentrations also show corresponding variation. The

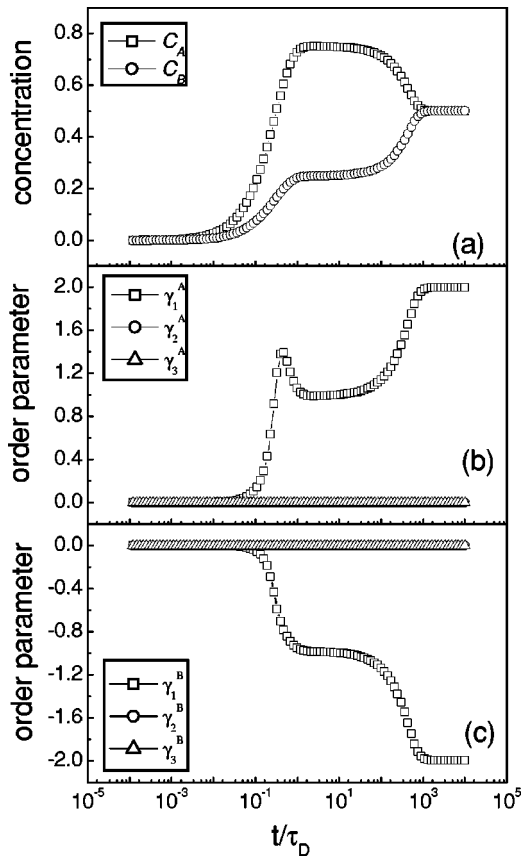


FIG. 6. Evolution of the structure parameters during the growth for the ordered phase $O_1$ at the temperature $k_BT=0.6$ and the chemical potentials $\mu_A=0.5$ and $\mu_B=0.25$. Here $w_A/\nu_D=1/8$ and $w_B/\nu_D=1/16$. (a) Curves for concentrations, (b) curves for $\gamma_1^A$, $\gamma_2^A$, and $\gamma_3^A$, and (c) curves for $\gamma_1^B$, $\gamma_2^B$, and $\gamma_3^B$.

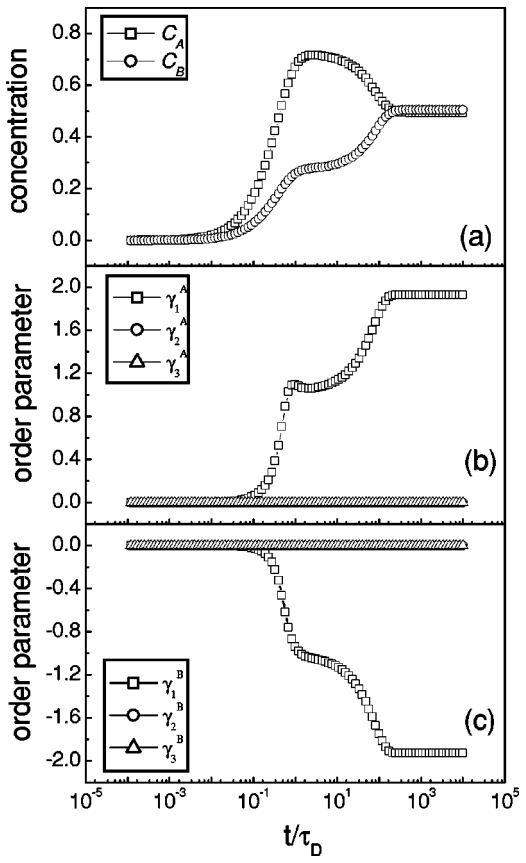


FIG. 7. Evolution of the structure parameters during the growth for the ordered phase $O_1$ at the temperature $k_BT=0.9$ and the chemical potentials $\mu_A=0.5$ and $\mu_B=0.25$. Here $w_A/\nu_D=1/8$ and $w_B/\nu_D=1/16$. (a) Curves for concentrations, (b) curves for $\gamma_1^A$, $\gamma_2^A$, and $\gamma_3^A$, and (c) curves for $\gamma_1^B$, $\gamma_2^B$, and $\gamma_3^B$.

concentrations of the species $A$ and $B$ approach to the steady values in the first stage of the growth process, which corresponds to the plateau of the curves shown in Fig. 6(a). The ratio between the two atomic concentrations satisfies relation (9). The concentration of each atomic species readjusts to reach the equilibrium values in the second stage of the growth process. The concentration of the species $A$ decreases after the plateau variation and the concentration of $B$ species changes in an opposite way. The equilibrium concentrations of $A$ and $B$ species can not be described by relation (9) because the equilibrium arises from a correlated effect of evaporation and adsorption. Now we make some analysis on the physical mechanism for this phenomenon. In the second stage, the coverage is almost full. The concentration of vacancy is very small and the atomic migration is slow. The variation of the order parameters is due to the readjustment of the atomic concentrations. With the increase of temperature, the evaporation rate becomes larger and the effect of evaporation on the kinetic process of the system becomes significant, especially in the case of a low concentration of vacancies. Therefore, this phenomenon is mainly due to the high evaporation rate at high temperature. The evaporation depends on the characteristic evaporation rate, chemical potentials, and bond broken factor. For the ordered phase $O_1$, the pair interaction favors the nearest-neighbor pairs of $A$ and $B$ atoms and second-nearest-neighbor pairs of the same kinds of atoms. After the first stage of the growth process, there are more $A$ atoms on the $\alpha$ and $\beta$ sublattices and more $B$ atoms on the $\gamma$ and $\delta$ sublattices. As a result, the $A$ atoms on the $\gamma$ and $\delta$ sublattices are easier to evaporate than the $B$ atoms due to the smaller broken bond energy with the $A$ atoms on the $\alpha$ and $\beta$ sublattices. This leads to a decrease of the concentration of $A$ atoms and an increase of the concentration of $B$ atoms. As feedback, $A$ atoms on the $\alpha$ and $\beta$ sublattices are more difficult to evaporate and the site probabilities of $A$ atoms on the $\alpha$ and $\beta$ sublattices increase. Therefore, the order parameters increase in the second stage of the growth process. In brief, the first stage of the growth process is determined by the adsorption and atomic exchange processes and the second stage of the growth process is controlled by the evaporation process. Figure 7 shows the evolution process for the temperature $k_BT=0.9$. In comparison with Fig. 6, the period of the first stage is reduced. Since the evaporation effect is more significant, the period of the first stage decreases with the increase of temperature. The order parameters of the ordered phase in the second stage of the growth process decrease due to the entropy-induced disordering. We can define the lifetime of the metastable ordered state as $\tau_m=t|_{C_A=(C_m+C_e)/2}-t|_{C_A=C_m/2}$, where $C_m$ is the maximal concentration of the species $A$ for the metastable ordered

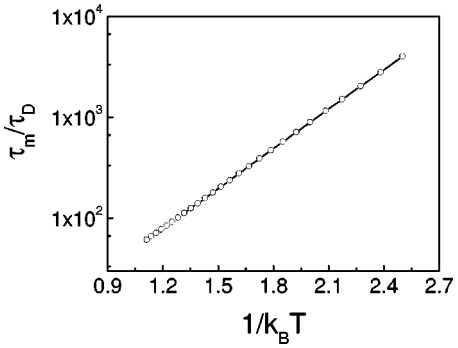


FIG. 8. The lifetime of the transient ordered state as a function of the reciprocal of temperature.

state. $C_e$ is the concentration of the species $A$ for the equilibrium state. Figure 8 shows the lifetime of the metastable ordered state in the first stage of the growth process as a function of the reciprocal of temperature. It can be seen that the life time of the metastable ordered state is exponentially proportional to the reciprocal of temperature.

### C. Effect of chemical potentials

We have investigated the evolution of the system with the variation of the chemical potentials. Figure 9 shows the evolution process for the chemical potentials $\mu_A=0.08$ and $\mu_B=0.05$ which are smaller than those of Fig. 7. In comparison with Fig. 7, it can be seen that the time period for the system to enter into the first stage of the growth process become longer and the lasting time of the plateau region in the first stage is reduced. Thus the relaxation time of the first and second stages of the growth process is reduced. When the chemical potentials are decreased, and the adsorption rate decreases, which makes the growth process slower. The decrease of the chemical potentials also makes the effect of the evaporation on the growth process stronger. In the second stage, the stronger evaporation effect makes the system relax to the equilibrium state faster.

## IV. SUMMARY

We have investigated the kinetics of ordering during the growth of a (001) monolayer in fcc alloy. The evolutions of the structure are calculated. There is a transient ordered state during the growth process due to the correlated effect of the atomic migration and adsorption. The occurrence of the transient ordered state depends on the ratio of the characteristic atomic exchange rate to the characteristic evaporation rate. There are two stages of the evolution in the growth process. The first stage of the growth process is the evolution of metastable ordered state. The second stage of the growth process is the kinetic process from the metastable ordered state to the equilibrium ordered phase. The lifetime of

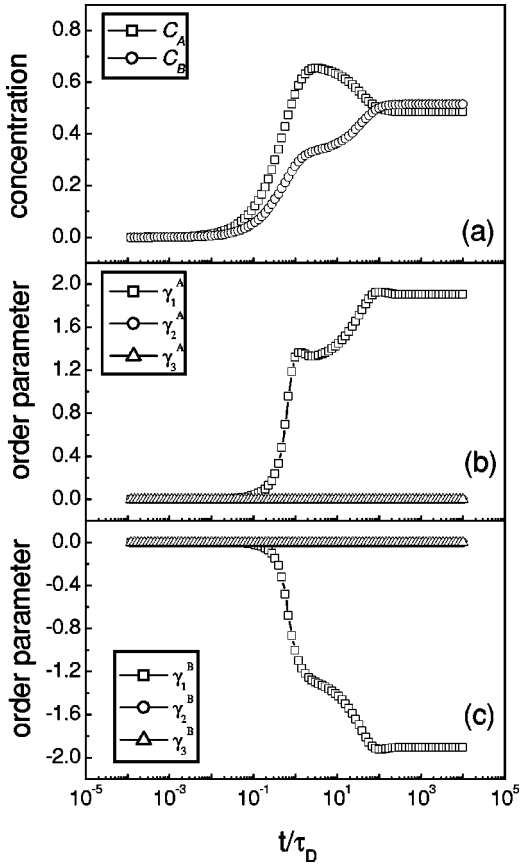


FIG. 9. Evolution of the structure parameters during the growth for the ordered phase $O_1$ at the temperature $k_BT=0.9$ and the chemical potentials $\mu_A=0.08$ and $\mu_B=0.05$. Here $w_A/\nu_D=1/8$ and $w_B/\nu_D=1/16$. (a) Curves for concentrations, (b) curves for $\gamma_1^A$, $\gamma_2^A$, and $\gamma_3^A$, and (c) curves for $\gamma_1^B$, $\gamma_2^B$, and $\gamma_3^B$.

the metastable ordered state decreases with the increase of temperature. The first stage of the growth process is mainly controlled by the adsorption and the atomic exchange process. The ratio of the concentration of the two atomic species for the metastable ordered state is given by $C_A/C_B=w_A\exp(\mu_A/k_BT)/w_B\exp(\mu_B/k_BT)$. The lifetime for the metastable ordered state increases exponentially with the decrease of the temperature. The second stage of the growth process is mainly governed by the evaporation and the atomic exchange process. The evaporation and the adsorption rate depend on the chemical potentials of the atomic species. For the case of large chemical potentials, the evaporation is weak and adsorption is the controlling effect. With the decrease of the chemical potentials, the evaporation is more effective. Thus the decrease of the chemical potentials has a similar effect as the increase of temperature.

## ACKNOWLEDGMENTS

This research was supported by the National Key Program of Basic Research Development of China under Grant No. G2000067107) and the National Natural Science Foundation of China under Grant No. 19804007.

[1] T.S. Kuan, T.F. Kuech, W.I. Wang, and E.L. Wilkie, Phys. Rev. Lett. **54**, 201 (1985).
[2] G.B. Stringfellow and G.S. Chen, J. Vac. Sci. Technol. B **9**, 2182 (1991).
[3] J.E. Bernard, S. Froyen, and A. Zunger, Phys. Rev. B **44**, 11 178 (1991).
[4] A. Zunger and S. Mahajan, in *Handbook on Semiconductors*, edited by T.S. Moss and S. Mahajan (Elsevier, Amsterdan, 1994), Vol. 3, p. 1399.
[5] B.L. Gu, Z.F. Huang, J. Ni, J.Z. Yu, K. Ohno, and Y. Kawazoe, Phys. Rev. B **51**, 7104 (1995).
[6] C. Ern, W. Donner, H. Dosch, B. Adams, and D. Nowikow, Phys. Rev. Lett. **85**, 1926 (2000).
[7] J.A. Pitney, I.K. Robinson, I.A. Vartaniants, R. Appleton, and C.P. Flynn, Phys. Rev. B **62**, 13 084 (2000).
[8] Y. Saito and H. Müler-Krumbhaar, J. Chem. Phys. **70**, 1078 (1979).
[9] R. Venkatasubramanian, J. Mater. Res. **7**, 1235 (1992).
[10] J.R. Smith and A. Zangwill, Phys. Rev. Lett. **76**, 2097 (1997).
[11] C.D. Adams, D.J. Srolovitz, and M. Atzmon, J. Appl. Phys. **74**, 1707 (1993).
[12] Y. Saito and H. Müller-Krumbhaar, Phys. Rev. Lett. **74**, 4325 (1995).
[13] M. Ishimaru, S. Matsumura, N. Kuwano, and K. Oki, Phys. Rev. B **51**, 9707 (1995).
[14] M. Kotrla and M. Predota, Europhys. Lett. **39**, 251 (1997).
[15] L.Q. Chen and A.G. Khachaturyan, Phys. Rev. B **44**, 4681 (1991).
[16] L. Reinhard and P.E.A. Turchi, Phys. Rev. Lett. **72**, 120 (1994).
[17] J. Ni, B.L. Gu, T. Ashino, and S. Iwata, Phys. Rev. Lett. **79**, 3922 (1997).
[18] J. Ni and B.L. Gu, J. Chem. Phys. **113**, 10 272 (2000).
[19] L.Q. Chen and J.A. Simmons, Acta Metall. Mater. **42**, 2943 (1994).
[20] A.S. Bakai and M.P. Fateev, Phys. Status Solidi B **158**, 81 (1990).